

[Article]

Classification of the Steady Axisymmetric Vortices

TAKAHASHI Koichi

Abstract : It has been shown that the Navier-Stokes equation for steady axisymmetric vortices is equivalent to a one-dimensional classical mechanics of a mass point subjected to non-conserved as well as conserved force. This equivalence is manifested by the ν -expansion method and makes it possible to survey new class of vortex solutions in addition to the Burgers' and the Sullivan's ones. The solutions are classified into three types according to how the mass point behaves in the potential before the asymptote is approached. Each type has a distinct cell number. All of the solutions are mutually connected by a continuous route in the parameter space. A non-local constant common to these solutions is presented.

Keywords : Navier-Stokes equation, ν -expansion, sequence of vortices

1. Introduction

The motion of fluid is modeled by the NS equation that is expressed as

$$\partial_t \mathbf{v} + \mathbf{v} \cdot \nabla \mathbf{v} = \nu \nabla^2 \mathbf{v} - \frac{\nabla \rho}{\rho} + f \quad (1)$$

with the obvious notations. There exist two one-parameter steady axisymmetric vortex solutions whose analytic forms have been exactly known : one was found by Burgers (1948) and the other by Sullivan (1959). It is customary to discriminate these two solutions by the number of the 'cells' that are characterized by the direction of the flow. Burgers' vortex has one cell and Sullivan's vortex has two.

Recently, it was found that there exist other steady axisymmetric vortex solutions than Burgers' and Sullivan's ones by noticing an analogy between the vortex system and a mass point subjected to non-conserved as well as a conserved force (Takahashi 2014). This analogy was noticed through the ν -expansion method in which the velocity field and the pressure are assumed to be subjected to the Taylor expansion in ν , thereby deriving a set of equations among the expansion coefficients.

In this paper, we first review the method that enable us to translate the vortex flow dynamics to the dynamics of a mass point and then find the complete list of the types of the steady axisymmetric vor-

tex solutions that connect the Burgers' and the Sullivan's vortices.

2. ν -expansion method and the NS equation

In the ν -expansion method it is assumed that the velocity field and the pressure are subjected to the asymptotic expansion in ν . For the present purpose, we write in cylindrical coordinate as

$$v_r = \nu v_{r1}, \quad (2.1)$$

$$v_\theta = v_{\theta 0}, \quad (2.2)$$

$$v_z = \nu v_{z1}, \quad (2.3)$$

$$p = p_0 + \nu^2 p_2, \quad (2.4)$$

that are suggested by the invariance of the NS equation under $\nu \rightarrow -\nu$. Namely, for v_r and v_z , terms higher than ν^1 vanish. For v_θ , terms higher than ν^0 vanish. For p , terms higher than ν^2 vanish. This parameterization implies that, in inviscid limit, v_r and v_z vanish, and v_θ and p remain finite.

Substituting these to (1) and equating the coefficients of terms with the same order of ν , we have the following equations for steady axisymmetric solutions.

(i) $O(\nu^0)$

$$-\frac{v_{\theta 0}^2}{r} + \frac{1}{\rho} \partial_r p_0 - f_r = 0, \quad (3.1)$$

$$\frac{1}{\rho} \partial_z p_0 - f_z = 0. \quad (3.2)$$

(ii) $O(\nu^1)$

$$\frac{v_{r1}}{r} \partial_r (r v_{\theta 0}) = \nabla^2 v_{\theta 0} - \frac{v_{\theta 0}}{r^2}, \quad (3.3)$$

$$\frac{1}{r} \partial_r (r \rho v_{r1}) + \partial_z (\rho v_{z1}) = 0. \quad (3.4)$$

(iii) $O(\nu^2)$

$$v_{r1} \partial_r v_{r1} + \frac{\partial_r p_2}{\rho} = \nabla^2 v_{r1} - \frac{v_{r1}}{r^2}, \quad (3.5)$$

$$v_{r1} \partial_r v_{z1} + v_{z1} \partial_z v_{z1} + \frac{\partial_z p_2}{\rho} = \nabla^2 v_{z1}. \quad (3.6)$$

(3.4) is the continuity equation. There are six equations for five unknown functions. (3.1) and (3.2) will be used to determine the r and z dependences of p_0 provided that the form of f allows consistent solutions. (3.3) is used to solve for $v_{\theta 0}$ once v_{r1} is given. (3.4), (3.5) and (3.6) can be used to determine v_{r1} , v_{z1} and p_2 .

3. Steady vortex solutions

Let us seek solutions in which v_{r1} and $v_{\theta0}$ do not depend on z . The simplest way to obtain such solutions is to assume (Burgers 1948, Sullivan 1959)

$$\frac{\partial_z p_2}{\rho} = -4k^2 z, \quad (4.1)$$

$$v_{z1} = -x(r)z, \quad (4.2)$$

where k is an arbitrary constant and x is a function of r only.

Consider first (3.3), which is rewritten as

$$v_{\theta0}'' + \left(\frac{1}{r} - v_{r1}\right)v_{\theta0}' - \left(\frac{1}{r^2} + \frac{v_{r1}}{r}\right)v_{\theta0} = 0. \quad (5)$$

The prime denotes the derivative with respect to r . It should be noted that, even in the absence of boundary, the inviscid flow $v_{\theta0}$ is affected from the viscous component v_{r1} . The general regular solution is given by

$$v_{\theta0} = \frac{C}{2\pi r} \int_0^r dr r e^{\int^r dr' v_{r1}(r')}. \quad (6)$$

C is a constant. In order for $v_{\theta0}$ to be finite at infinity, $v_{r1}(\infty)$ must be negative.

Next consider (3.4) and (3.5). From the continuity (3.4), we have

$$v_{z1} = -\frac{z}{r}(rv_{r1})'. \quad (7)$$

(7) and (4.2) lead to

$$v_{r1} = \frac{1}{r} \int_0^r x r dr. \quad (8)$$

On the other hand, substituting (7) into (3.6), together with (4.1), yields

$$v_{r1}''' + \left(\frac{2}{r} - v_{r1}\right)v_{r1}'' - \left(\frac{1}{r^2} - \frac{v_{r1}}{r} - v_{r1}'\right)v_{r1}' + \frac{v_{r1}}{r^3} + \frac{2v_{r1}^2}{r^2} = 4k^2. \quad (9)$$

For $k \neq 0$, there exist solutions of (9) that behave as $v_{r1} \propto r$ near $r = 0$. Thus far two solutions are known (k is chosen to be positive)

$$v_{r1,B} = -kr, \quad (10.1)$$

$$v_{r1,S} = -kr + 6(1 - \exp(-kr^2/2))/r. \quad (10.2)$$

The former and the latter are due to Burgers (1948) and Sullivan (1984), respectively.

Note that v_r vanishes in the inviscid limit, while v_{r1} remains effective in determining the observable v_{θ} through (6). This is the phenomenon called the Cheshire cat effect in Takahashi (2014).

4. Equivalent mass point motion

An insight into the possible global behaviours of the solutions of (9) is gained by rewriting it in terms of the variable x introduced by (4.2). Together with (7), (9) takes the form

$$x'' = -x^2 + 4k^2 + \left(v_{r1} - \frac{1}{r}\right)x'. \tag{11}$$

If we reinterpret r as the ‘time’ and x as the ‘coordinate’ of a particle with a unit mass, then this equation describes a classical one-dimensional motion of the mass point in the potential $U(x) = x^3/3 - 4k^2x$ under the effect of a non-conservative force given by the last term on the r.h.s. of (11). An example of the form of the potential U is depicted in Fig.1 for $4k^2 = 1$. (This is equivalent to rescale the variables as $x \rightarrow 2kx$, $r \rightarrow r/(2k)^{1/2}$ in (11).)

Multiply the both sides of (11) by x' and rewrite the resultant equation to obtain

$$\frac{d}{dr} \left(\frac{x'^2}{2} + U(x) \right) = \left(v_{r1} - \frac{1}{r} \right) x'^2. \tag{12}$$

This equation expresses how the particle’s ‘total energy’ temporally varies under the presence of the non-conservative force. If the l.h.s. of (12) is zero, then the energy is conserved. This situation is achieved by resting the mass point at one of the extrema of the potential. Discarding the positive value by the reason already mentioned, the acceptable solution is

$$x = -1 \text{ or } v_{r1} = -\frac{r}{2}. \tag{13}$$

This is depicted as A in Fig. 1, which is nothing but the Burgers vortex solution (10.1) with the energy of the mass point equal to $2/3$. We require any physical solution to asymptotically approach the position A in order to avoid too rapid a divergence of the velocity field at $r = \infty$.

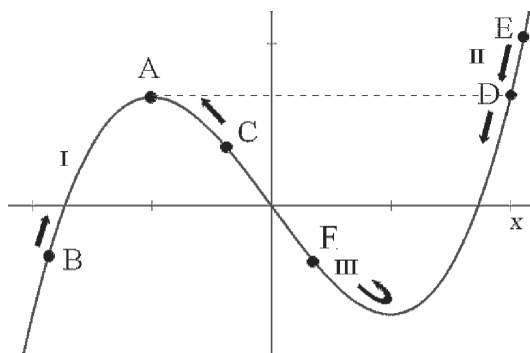


Fig. 1 Potential $U = x^3/3 - 4k^2x$, with $4k^2 = 1$. The maximum and minimum points are $x = -1$ and 1 , respectively. This graph shows why $k^2 > 0$ is necessary for physical solutions to exist. For alphabetical letters, arrows and Roman numerals, see the text.

The mass point at rest at a position other than the extrema begins to roll down the potential slope. The mass point loses the energy due to the dissipative term $-x'^2/r$ that is initially dominant. Even in the case v_{r1} temporarily acquires positive values, on approaching the point A, the functional form of v_{r1} should approach $-r/2$, thereby the non-conservative force eventually turns totally dissipative. By appropriately choosing the initial position, the mass point will approach A at $r = \infty$. Such a motions corresponds to the Sullivan's vortex, for which $x(0) = 2$. This point is designated by D in Fig. 1. Its initial energy is $2/3$, being equal to the final energy.

When the initial position is B in Fig. 1, then the mass point can climb up the slope if the acceleration $x''(0)$ has a positive sign at B. By appropriately choosing the acceleration, the mass point will be in the stationary state A at $r = \infty$ (Type I solutions). This is easily confirmed by numerical calculation, in which the 'initial time' is chosen as r_0 , slightly off the point $r = 0$. The similar thing holds for C with negative initial acceleration.

Solutions whose initial position is near D, like E in Fig. 1, can approach the point A if the initial acceleration is of an appropriate negative value (Type II solutions).

It is conjectured that the mass point at the initial point C or F may have a positive initial acceleration, i.e., $x''(r_0) > 0$, to reach the point A at $r = \infty$. In this case, the mass point will move down the slope and then up the opposite slope beyond the local minimum, stops at a certain point $x = x_{\max} > 1$, turns the direction of motion and goes down and then climbs up toward the point A (Type III solutions). The peculiar characteristics of such motions for the points C and F will be entirely due to the existence of v_{r1} in the non-conservative force of our fictitious classical dynamics.

Prominent aspects of these solutions are that $x(r_0) \rightarrow -\infty$ as $r_0 \rightarrow 0$ for of Types I and III and $x(r_0) \rightarrow +\infty$ for Type II. In fact, (11) has a class of solutions that are expanded around $r = 0$ as

$$x(r) = \sum_{m=n=0}^{\infty} a_{m,n} (\ln r)^m r^{2n}, \quad (14)$$

where $a_{m,n}$ are determined from $a_{0,0}$ and $a_{1,0}$ as

$$a_{1,1} = \frac{a_{1,0}^2}{8} - \frac{a_{0,0}a_{1,0}}{2}, \quad a_{0,1} = \frac{1 - a_{0,0}^2 - a_{1,0}^2}{4} + \frac{5a_{0,0}a_{1,0}}{8}, \quad a_{2,0} = a_{2,2} = 0, \dots \quad (15)$$

$a_{0,0}$ and $a_{1,0}$ must be chosen so as for $x(r)$ to asymptotically approach -1 . For a given $x(r)$, v_{r1} and v_{z1} are determined by (4.2) and (7). We must restrict m to be 0 or 1.

$x(r)$ generally has a logarithmic singularity at $r = 0$, which gives rise to the same type of singularity in v_{r1} . Importantly, it gives rise to no divergence in the fluxes of such observable quantities as momentum or energy. This means that $x(r)$'s given by (14) with $a_{1,0} \neq 0$ also are physically acceptable solutions.

5. Numerical calculations

$a_{1,0}$ for Types I and III solutions is positive, while for Type II it is negative. The components v_{r1} and v_{z1} of our solution for particular choices of $(a_{1,0}, a_{0,0})$, together with the Burgers and Sullivan solutions, are shown in Fig. 2.

The zeros of v_{r1} and v_{z1} for the solutions of Types II and III are evident in Fig. 2. Besides, for the solution of Type III, there exists one more zero very near $r = 0$ because of the leading $\ln r$ term. In the terminology of Sullivan (1959), the solutions of Types II and III have a two- and three-cell structure, respectively. The innermost cell of the solution of Type III may be too small to have any significant meteorological meanings. (The motion F in Fig. 1 belongs to Type III. In the corresponding figure in Takahashi (2014), the motion denoted by F was noticed to have two cells. It was due to that the initial time ' r_0 ' chosen in numerical calculations was not sufficiently small. The motion F is in fact of three cell structure if r_0 is chosen to be small enough.)

The pairs of $a_{1,0}$ and $a_{0,0}$ that permit the solution x with the correct boundary condition form a spiral-like structure as is shown in Fig. 3(a). The curve is divided into three parts with distinctive characters. In Fig. 3(a), each part is labeled as I, II or III according as which of the solutions shown in

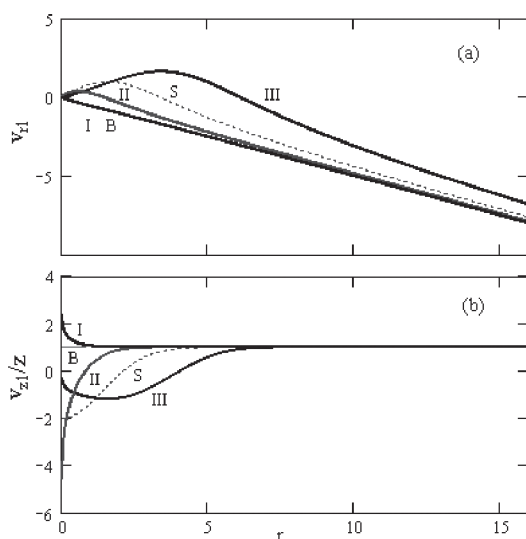


Fig. 2 r -dependences of (a) v_{r1} , (b) v_{z1}/z for three possible solutions denoted by I, II and III, each of which is a representative of solutions of Type I, II and III, respectively. Parameters $(a_{1,0}, a_{0,0})$ for the drawn curves are I: $(0.41, -0.818)$, II: $(-1.09, 0.266)$, III: $(0.2, 1.072)$. For references, the Burgers solution (B) and the Sullivan solution (S) are also depicted by broken line ($v_{r1} = 1$) and dotted curve, respectively. v_{r1} of the solution I almost coincides with that of the Burgers solution.

Fig. 2 belongs to. The point $(a_{1,0}, a_{0,0}) = (0, -1)$ corresponds to the Burgers solution. The point $(0, 2)$ corresponds to the Sullivan solution.

The limit $a_{1,0} \rightarrow 0$ on the part III leads to another distinct point $(0, 1)$, which has no correspondence to the solution of the NS equation. This is because the minimum point of the potential $U(x)$ is essentially different from any nearby points. The mass point with zero velocity and zero acceleration at the minimum point can never go up the slope. Oppositely, the mass point at a position slightly off the minimum of U slips down the potential slope and then goes up the opposite slope. If the time during which $v_{r1} > 0$ is appropriately adjusted, the mass point can gain sufficient energy to reach the maximum of U . For this class of solutions, the region in which $v_{r1} > 0$ becomes larger and larger when $a_{1,0}$ approaches 0.

For a given $a_{1,0}$, there exist two Type III solutions. These are discriminated by the value of x_{\max} as is shown in Fig. 3(b).

$v_{\theta 0}$ is determined by (6) and is shown in Fig. 4 together with those of the Burgers and Sullivan solutions. Far away from the maximum point, $v_{\theta 0}$ decreases as $1/r$. Near the symmetry axis, $v_{\theta 0}$ is proportional to r for all three flows. However, the rates of the subsequent rise are different : because of a large region of positive v_{r1} , $v_{\theta 0}$ of the solution III increases relatively very rapidly with r , thereby

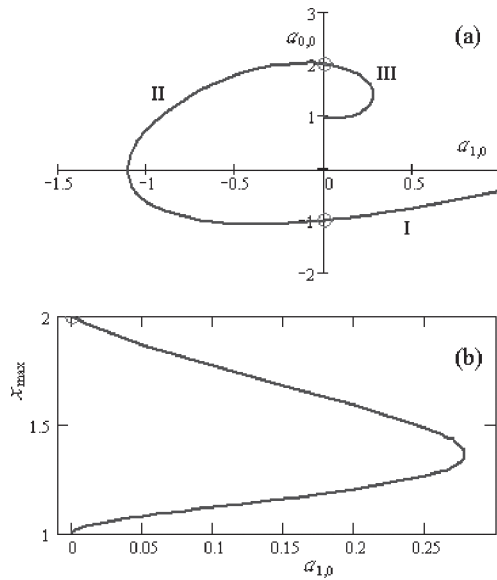


Fig. 3 (a) Spiral-like structure of the parameter set $(a_{1,0}, a_{0,0})$ that yields the vortex solution. Three parts in the set designated by I (the fourth quadrant), II (the second and the third quadrants) and III (the first quadrant). Circles at $(0, -1)$ and $(0, 2)$ give the Burgers and Sullivan solution, respectively. (b) Maximum values of x for the type III solutions.

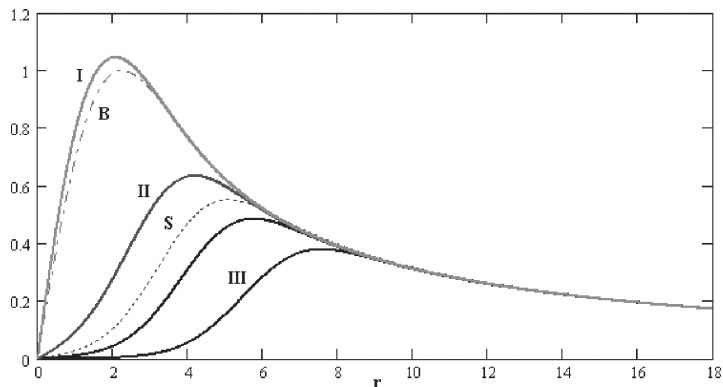


Fig. 4 $v_{\theta 0}$ determined by (6). The solid curves labeled I, II and III are calculated from the corresponding solutions I, II and III in Fig. 2. Broken curve and dotted curve are the Burgers (labeled by ‘B’) and Sullivan (labeled by ‘S’) solution, respectively. The unlabeled curve is also of Type III with the parameters $(a_{1,0}, a_{0,0}) = (0.2, 1.785)$. All curves are normalized so as to have an equal circulation at infinity.

forming a distinct ‘eye’ region. The eye region of Type III solution becomes larger as $a_{1,0}$ approaches 0. Larger eye region implies smaller peak of $v_{\theta 0}$ when the circulation at infinity is fixed. In the limit $a_{1,0} \rightarrow 0$, $v_{\theta 0}$ with fixed circulation vanishes. In this sense, the vortex loses energy and decays along the sequence I \rightarrow Burgers \rightarrow II \rightarrow Sullivan \rightarrow III \rightarrow O, where ‘O’ stands for absence of vortex.

For finite ν , νv_{r1} , $v_{\theta 0}$ and νv_{z1} give the vortex structure. The radial direction of the flow of the Types II and III changes near the middle point of the ‘eye-wall’ where $\partial_r v_{\theta 0}$ is positive and large. In the outer and inner regions, separated from each other by the eye-wall, the flow directs inward and outward, respectively. In inviscid limit, only the azimuthal component remains.

The equation (12) suggests that the non-local quantity C defined by

$$C \equiv \frac{1}{2}x'^2 + U(x) + \int_n^r \left(\frac{1}{r} - v_{r1} \right) x'^2 dr \tag{16}$$

is a constant : it does not depend on r for all types of vortices. Choosing $r_1 = +\infty$ and recovering the freedom of the parameter k , C takes a universal value $(2/3)4k^2$ for all the solutions. By construction, C does not depend on ν , too. What discriminates the types of vortices may be the cell number, n_c , or the frequency n_m that the orbit $x(r)$ visits the local minimum of $U(x)$ as r varies from 0 to ∞ . n_c and n_m are related by $n_c = n_m + 1$. $(n_c, n_m) = (1, 0)$, $(2, 1)$ and $(3, 2)$ for Type I, II and III vortices, respectively. On the other hand, $(n_c, n_m) = (1, 0)$ for the Burgers’ vortex and $(2, 1)$ for the Sullivan’s vortex, as is tabulated in Table 1.

What discriminates the Type I and Burgers solutions is the initial value of x , i.e., $x(0) = -\infty$ and

Table 1 Continuous sequence of the vortex solutions. ‘O’ represents no solution.

	Type I	Burgers	Type II	Sullivan	Type III	O
n_c	1	1	2	2	3	—
n_m	0	0	1	1	2	—
$x(0)$	$-\infty$	-1	$+\infty$	1	$-\infty$	—

-1 for the former and the latter, respectively. $x(0)$ for other solutions are also given in Table 1.

6. Summary

By solving a closed set of equations derived in the lowest order of the ν -expansion scheme, we found all the steady and axisymmetric vortex solutions for the NS equation that connect the Burgers’ and the Sullivan’s solutions. These solutions called Type I, II and III consist of one, two and three cells, respectively, and involve the Burgers and Sullivan vortices as the special cases. The innermost cell of Type III vortex is very small. Its astrophysical implication may be worth exploration. We also found the route in the parameter space along which the steady and axially symmetric vortex continuously changes itself along the following sequence : Type I \rightarrow Burgers \rightarrow Type II \rightarrow Sullivan \rightarrow Type III \rightarrow O. When the circulation at infinity is kept constant, this route represents the sequence of the decay of the vortex. The flow profiles in the inviscid limit are uniquely determined. It remains as an open question whether the Donaldson-Sullivan’s vortex solution (Baker 2000) is similarly extended.

References

- Baker J T 2000 High viscosity solutions of the Navier-Stokes equations modeling a tornado vortex *Thesis in mathematics, the graduate faculty of Texas Tech. Univ.* ;
<https://repositories.tdl.org/ttu-ir/bitstream/handle/2346/18824/31295016657479.pdf?sequence=1>.
 Burgers J M 1948 A mathematical model illustrating the theory of turbulence *Adv. Appl. Mech.* **1** 171.
 Sullivan R D 1959 A two-cell vortex solution of the Navier-Stokes equations *J. Aerosp. Sci.* **26** 767.
 Takahashi K 2014 Non-Euclidian inviscid vortices *Fac. Lib. Arts Rev. (Tohoku Gakuin Univ.)* **167** 43.
http://www.tohoku-gakuin.ac.jp/research/journal/bk2014/pdf/no01_04.pdf.